

Hydrostatic instabilities in floating zone crystal growth process

J. Meseguer, J. M. Perales, I. Martínez, N. A. Bezdenejnykh and A. Sanz

IDR/UPM. E.T.S.I. Aeronáuticos, Universidad Politécnica de Madrid. 28040 Madrid, Spain

ABSTRACT

If only Fluid Mechanics aspects are considered, the configuration appearing in the floating zone technique for crystal growth can be modelled as a mass of liquid spanning between two solid rods. Besides, if now the influence of temperature gradients and heat flow are not considered, the simplest fluid model consists of an isothermal liquid mass of constant properties (density and surface tension) held by capillary forces between two solid disks placed a distance L apart: the so called liquid bridge. As it is well known, if both supporting disks were parallel, coaxial and of the same diameter, $2R$, the volume of liquid, V , were equal to that of a cylinder of the same L and R ($V=\pi R^2 L$) and no body forces were acting on the liquid column, the fluid configuration (under these conditions of cylindrical shape) will become unstable when the distance between the disks equals the length of the circumference of the supporting disks ($L=2\pi R$, the so-called Rayleigh stability limit). One should be aware that the Rayleigh stability limit can be dramatically modified when the geometry differs from the above described cylinder (due to having non-coaxial disks, different diameter disks, liquid volume different from the cylindrical one, etc) or when other external effects like accelerations either axial or lateral are considered.

In this paper the stability limits of liquid bridges considering different types of perturbations are reviewed. Available numerical and experimental results, which cover a broader range of parameter variation, as well as analytical expressions for these limits, obtained using asymptotic analyses, are presented.

1. INTRODUCTION

In many practical situations in crystal growth

processing, to obtain material of high and controllable purity, it is necessary to fabricate the crucible from material that is not chemically attacked by the molten charge. This is not always possible, as it happens with rare earth metals, and in this situation, when the contact between the crucible and the melt must be avoided, the floating zone technique is an alternative. With this technique, shown schematically in Fig. 1, a molten zone is established between two rods: a charge or feed rod of polycrystalline material and a monocrystalline rod. The molten zone can be established in a variety of ways depending on the material to be crystallised; for example radio frequency induction heating using a single turn coil or radiation heating in mirror furnaces are commonly used with silicon whereas electron beam melting is employed in the case of refractory metals [1, 2, 3]. To maintain axial thermal symmetry and to exert

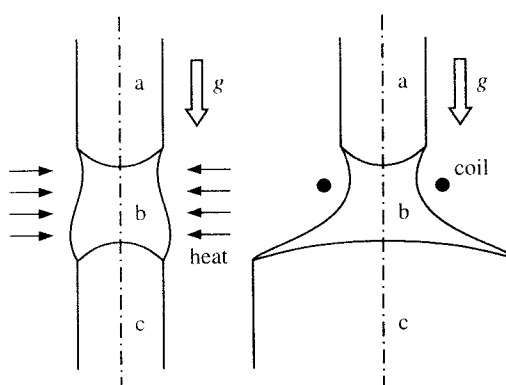


Fig. 1. Sketch of the configuration appearing in the floating zone process of crystal growth: a) feed rod, b) molten zone, c) crystalline rod.

some control over the shape of the solid-liquid interfaces, the crystal and charge rods are rotated.

On earth, gravitational forces set an upper limit to the molten zone length and therefore to the crystal diameter, so that rods of only a few millimeters in diameter could be zoned thereby. However, refinements of the floating zone technique based on a precise knowledge of the behaviour of the liquid phase allow the growing of cylindrical shaped crystals with diameters of several centimeters [2]. In this case typically an induction-heating pancake coil is used with a diameter smaller than that of the crystal; the upper feed rod melts to a conical shape, with the melt running down through the induction coil. The melt collects in a puddle and freezes onto the growing crystal below. The electromagnetic field of the induction heating coil helps to support the molten zone.

As it is well known, crystal growth process by using the floating zone technique consists of the following steps:

- 1) Melt-drop generation at the ends of a seed and a feed rod,
- 2) Joining of the melts,
- 3) Necking to obtain dislocation-free material,
- 4) Diameters increase, and
- 5) Full-diameter zone growth.

In this process, heating as well as the relative speed between the heating source and the rod have to be carefully adjusted for each step to maintain the desired zone lengths and diameters within stable limits to avoid the dripping down of the zone (heating power too high) or growing together of seed and feed rod in the middle of the zone (power too low or speed too high).

Therefore, in the floating zone process, due to either the growing process itself or to non-desired perturbations, a large variety of melt shapes can appear. The melt can be between solid rods of equal or unequal diameters, it can be rotated, the supporting rods can be aligned or not aligned, etc., so that a precise knowledge of the behaviour of the hydrostatic stability of these melt shapes is of interest in order to prevent either the breaking of the melt zone or the growing of crystal having undesired shapes. This is of interest not only for the floating zone technique, but for other similar crystal growth techniques in which a melt drop spanning between two solid supports has to be handled (as it also happens in the Stepanov technique for the growth of

cylindrical crystals and other related techniques [1, 4, 5])

The equilibrium shapes and stability limits of the floating zone melt under the large variety of disturbances that could arise either accidentally or intentionally during the growing process is a matter of great concern. Its study involves a formidable task both because of the material characteristics of the melt, whose properties are strongly temperature dependent, and because of the complexities associated to the disturbances which could be imposed on the zone. Thence, several simplifications must be introduced in the model. The simplest approach consists in disregarding phase changes, considering a liquid zone held between two parallel solid disks, the so-called liquid bridge problem [6, 7, 8].

The liquid bridge is a relevant fluid configuration for its own merit as a simple and controllable setup for basic fluid science studies and for its direct application to the floating-zone crystal growth technique. As already said, in the simplest configuration a liquid bridge consists of an isothermal drop of liquid held by surface tension forces between two parallel, solid disks as shown in Fig. 2. Disregarding additional electric and magnetic fields effects, the equilibrium interface shape and hydrostatic stability limits of such a fluid configuration are determined by the following dimensionless

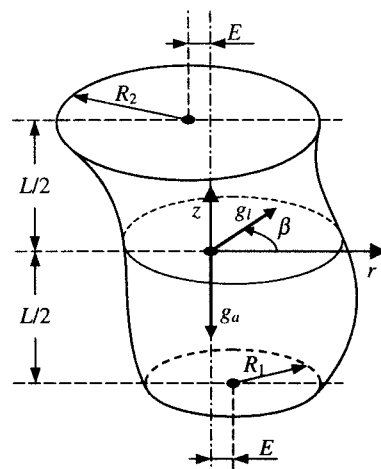


Fig. 2. Sketch of the liquid bridge configuration.

parameters:

- The slenderness, $\Lambda=L/(2R_0)$, where L is the distance between the supporting disks and $R_0=(R_1+R_2)/2$ is the mean radius, which is used as characteristics length to make the description dimensionless.

- The ratio of the radius of the smaller disk, R_1 , to the radius of the larger one, R_2 , That is $K=R_1/R_2$, or the equivalent parameter

$$h = \frac{1-K}{1+K} = \frac{R_2 - R_1}{R_2 + R_1} \quad (1)$$

Note that in Fig. 2 the smaller disk has been plotted at the bottom, the larger disk at the top and the axial acceleration points towards the small disk. The reason for this election is that most of the published works on the liquid bridge problem deal with the behaviour of liquid bridges under microgravity conditions like the ones existing in orbital platforms. Since in a space platform the elsewhere intuitive concepts of top and bottom are misleading, in the literature, the parameter K is assumed to be the ratio of the radius of the smaller disk to the radius of the larger one (so that the range of variation of h is restricted to $0 \leq h \leq 1$) and the axial Bond number is considered to be positive when the acceleration vector points towards the smaller disk and otherwise, the reason behind being, as is explained in the following, that the former case yields to more stable liquid bridge configurations than the later.

- The dimensionless eccentricity, $e=E/R_0$, $2E$ being the distance between the disks axes.

- The dimensionless volume, defined as the ratio of the actual volume V^* to the volume of a cylinder of the same length L and diameter $2R_0$:

$$V = \frac{V^*}{\pi R_0^2 L} \quad (2)$$

- The axial Bond number,

$$B_a = \frac{\Delta \rho g_a R_0^2}{\sigma} \quad (3)$$

where $\Delta \rho$ is difference between the density of the liquid and the density of the surrounding medium, g_a is the axial component of the acceleration acting on the

liquid, and σ is the surface tension.

- The lateral Bond number,

$$B_l = \frac{\Delta \rho g_l R_0^2}{\sigma} \quad (4)$$

where g_l stands for the lateral component of the acceleration acting on the liquid, which forms an angle β with respect to the plane defined by the axes of the disks.

- The Weber number (assuming that the liquid bridge is rotating as a solid body with angular velocity ω):

$$W = \frac{\Delta \rho \omega^2 R_0^3}{\sigma} \quad (5)$$

Hence, a liquid bridge is the simplest idealisation of real configuration appearing in the floating zone technique used for crystal growth and purification of high melting point material. Equilibrium shapes and stability limits of capillary liquid bridges have been analysed from both the theoretical and the experimental point of view during the last decades, and many papers dealing with such fluid configurations have been published (reviews of the state of the art in the field as of the early nineties can be found in [9, 10]). In the next section the differences and similarities between liquid bridges and floating zones are outlined, and in following sections the stability limits of liquid bridges considering different geometrical configurations are presented.

2. FROM FLOATING ZONES TO LIQUID BRIDGES

Although the protruding solid ends (solid caps entering into the liquid section) have a major impact on the logistics of the heating and puling laws during real floating zone processing, they have minor importance for the internal motion (because it is surface driven) and no importance at all for the mechanical stability of the melt [8], so that, the liquid bridge model sketched in Fig. 2 can be used instead of the real molten zone of Fig. 1 for modeling mechanical behavior without significant errors. The similarities and differences between the two configurations (simplified liquid bridge and real floating zone) can be summarised as follows:

● **Statics:** the liquid bridge is assumed to be at complete thermodynamic equilibrium, whereas if the solid-liquid interface for the melt were in the true thermodynamic equilibrium it could be in any position, because it is indifferently stable. In practice, in the floating zone, the solid-liquid interface is fixed by application of a non-uniform temperature field, slightly heating the melt and cooling the supports over and below the fusion temperature, respectively. If the temperature difference is not large, fluid properties (surface tension and density) can be taken as constant. Even during actual processing, where temperature differences as large as 100 K in 1 cm may exist, the variation of properties with temperature and the motions they create are so mild [11] that the outer shape and its mechanical stability seem to coincide with those predicted by the constant-property liquid bridge quiescent model.

The problem of how good the model is in the description of the liquid-solid interaction is another issue. Because mechanical relaxation times are much shorter than thermal or diffusional ones, it can be anticipated that if the melt is suddenly shaken, the solid-liquid interfaces would remain the same (at least for short times). One important issue now is the behaviour of the triple (solid-liquid-gas) line. The liquid could then remain edge-attached to the solid, or could slip over the solid. Experiments show that the anchoring assumption is correct [12].

● **Dynamics:** the interest is on predicting the

eigenfrequencies and motions caused by imposed mechanical perturbations. The parameters that enter into the dynamic model of the liquid bridge (leaving aside geometry) are: surface tension, density and viscosity, and there is an ample choice of model fluids which show similar properties to those of the high temperature melts of interest. The same remark on boundary conditions as above apply.

● **Convection:** the interest is on thermocapillary convection, and besides the dynamical parameters mentioned above, thermal diffusivity and change of surface tension with temperature play the major role. A handicap of the model is that Prandtl numbers $Pr = \mu c_p / k$ (the ratio of viscous to thermal diffusivity) for melts of technological interest are of order $Pr = 10^{-2}$ whereas for transparent liquids used at ambient temperature for laboratory experiments on liquid bridges it is $Pr = 10$, that is three orders of magnitude different (see Table 1 for examples of melts and transparent fluids).

In any case, it must always be kept in mind that the variation of surface tension with temperature is very difficult to measure for real melts (at temperatures near 2000 K) and uncertainties even in the order of magnitude exists.

● **Diffusion:** although the study of segregation and transport of impurities is one of the major goals of experiments on the floating zone process, little effort has been paid up to now to its analysis using the liquid bridge model (with a binary mixture liquid).

Table 1. Properties of some important liquids on floating zone or liquid bridge research (from [8])

Material	Si (at T_f)	Ge (at T_f)	Water (at 298 K)	DMS 5 (at 298 K)
Melting temperature, T_f [K]	1690	1210	273	
Refractive index (at $\lambda = 0.6 \mu\text{m}$), n	opaque	opaque	1.33	1.40
Density, ρ [$\text{kg}\cdot\text{m}^{-3}$]	2530	5500	1000	920
Thermal expansion, α [K^{-1}]	1.4×10^{-4}	10^{-4}	2×10^{-4}	10^{-3}
Surface tension, σ [$\text{N}\cdot\text{m}^{-1}$]	0.800	0.600	0.074	0.020
$-\text{d}\sigma/\text{d}T$ [$\text{N}\cdot\text{m}^{-1}\cdot\text{K}^{-1}$]	3×10^{-4}	3×10^{-4}	1.7×10^{-4}	10^{-8}
Thermal conductivity, k [$\text{W}\cdot\text{m}^{-1}\cdot\text{K}^{-1}$]	0.67	0.71	0.6	0.12
Thermal capacity, c_p [$\text{J}\cdot\text{kg}^{-1}\cdot\text{K}^{-1}$]	1000	380	4200	1800
Thermal diffusivity, $a = k/\rho c_p$	2×10^{-6}	34×10^{-6}	14×10^{-8}	7×10^{-8}
Kinematic viscosity, ν [$\text{m}^2\cdot\text{s}^{-1}$]	35×10^{-8}	14×10^{-8}	10^{-6}	5×10^{-6}
Prandtl number, $Pr = \nu/a$	0.02	0.01	7	55

- Phase changes: this is genuine to the floating zone, and the liquid bridge model is assumed to not account for phase changes. However, using model substances as succinonitrile, which has a well-defined fusion point ($T_f=330$ K), or even sodium nitrate ($T_f=580$ K), both of which have transparent melts, will surely help to understand real floating zone processing at 2000 K.
- Electric and magnetic effects: electric and magnetic fields are applied in real floating zone processes to better control the shape or the internal motions in the melt, and they can be similarly applied in the liquid bridge configuration [13-17].
- Reactive processes: it is easily understandable that, working at 2000 K, every system must be considered reactive. For the same reason, it is difficult to think of a liquid bridge at 300 K as a good model to analyse chemical reactions of interest to the floating zone process, although the fact that a liquid bridge offers a highly controllable and free configuration will no doubt stimulate its use for chemical reaction research.

In spite of these differences, the similarities between floating zones and liquid bridges allows the use of the later as a suitable model for the hydrostatic problems involved in the former. As already said, the primary interest of most of the published papers on liquid bridge

stability is not directly on crystal growth but on the behaviour of liquids under reduced body force conditions (the reason likely being the possibilities the available experiment opportunities for fluid physics studies under microgravity conditions on board orbital platforms). This is why sometimes is surprising to find in the literature studies on liquid bridge stability covering some aspects of apparently little (or none) interest from the crystal growth point of view.

The hydrostatic stability of liquid bridges has been analysed in a large number of publications. Trying to summarize the state of the art and provide a quick reference and a pointer to the relevant reference, a brief review of the cases studied is presented in Table 2. The references have been categorized according to the type of perturbation considered and to the year of publication. It must be pointed out only those works published in open western literature and easily available are quoted in Table 2. There are also a remarkable number of publications in the Russian literature dealing with liquid bridges or related problems (many of these works are quoted in [28, 34, 44, 48, 53]) but they have not been referenced here due to the difficulty of obtaining copies of them.

Before pursuing further and taking into account the number of parameters involved in the problem and the

Table 2. Some published papers dealing with the hydrostatic stability of liquid bridges. A cross in the first five columns indicates the effect considered. Numbers in the last three columns indicate, grouped by decades, the paper numbers according to the list of references. Bold numbers indicate that experimental results are presented.

B_u	h	W	B_l	e	References		
					70's	80's	90's
					18, 19 , 20 , 21, 22, 23	24 , 25 , 26	27, 28
X						29, 30 , 31	32, 33 , 34
	X					35, 36	37
X	X					38, 39, 40	41, 42 , 43 , 44
		X				45, 46	47 , 48
X		X			49	50, 51	52
X	X	X					53
	X	X			54 , 55		
X			X		56		57, 58 , 59 , 60
			X	X			61, 62
X			X	X			63
X	X		X	X			64

wide range of values that they can take if arbitrary variations of them were considered, it is convenient to have in mind a more definite (and floating zone technique oriented) liquid bridge configuration. As it has been previously discussed, liquid bridges are uniquely defined by the set of parameters Λ , K , e , V , B_a , B_l and W , so that it is now of interest to bound the values of these parameters in a real floating zone process.

Obviously the maximum slenderness depends on the values of the other parameters involved. Concerning the ratio of the radius of the small disk to the radius of the larger one, $h=(1-K)/(1+K)$, this parameter can vary from $h=0$ to $h=1$. The extreme $h=0$ means that both solid supports are equal in diameter ($K=1$), whereas the second value ($h=1$) means $K=0$ ($R_2=0$), although in this case the resulting configurations cannot be properly considered as liquid bridges, but rather sessile or pendant drops depending on the sense of the Bond number.

In the floating zone process the dimensionless eccentricity, e , will be usually zero (that means coaxial solid supports) or extremely small.

Dimensionless volume is bounded, for every value of the slenderness, between the maximum volume and the minimum volume stability limits, defined in the following. These maximum volume and minimum volume stability limits depend in turn on the rest of parameters under consideration (K , e , B_a , B_l and W), so that the range of values of V can be rather different depending on the imposed perturbations. Experiments on crystal growth performed both on board orbital platforms and in sounding rockets [2, 7, 8], where body forces effects are almost negligible ($B_a=0$, $B_l=0$), show that the value of V usually ranges between $V=1$ and $V=2$. On earth, floating zones are less slender than in a microgravity environment, but concerning the dimensionless volume the same range of upper values still hold.

With respect to the value of the Bond number, either axial or lateral, once the material properties are fixed, the value of this dimensionless parameter, measuring the ratio of hydrostatic pressure to capillary pressure, depends on the square of the mean radius, $R_0=(R_1+R_2)/2$. Taking into account typical values of both the density and the surface tension taken from

Table 1, and considering a typical value for the mean radius $R_0=2.5 \times 10^{-3}$ m, it is obtained $|B_a| \approx 1$, except in the case of Silicon oil, that yields a higher value (but of the same order of magnitude) $|B_a| \approx 3$. Therefore $|B_a| \approx 1$ would be an appropriate value of reference for the axial Bond number. Concerning the lateral Bond number, in a real floating zone process the value of this parameter is usually zero or very small (crystals are grown vertically).

Finally, the value of the Weber number is also small; typical values of the rotation speed in floating zone process are so slow that $W \approx 10^{-3}$ could be a suitable value for the upper bound of this parameter.

3. EQUILIBRIUM INTERFACE SHAPES

Leaving apart electric and magnetic effects, equilibrium shapes of liquid bridges are described by the Young-Laplace equation, which in dimensionless variables reads:

$$M(F) + P - B_a z + B_l F \cos(\theta - \beta) + \frac{1}{2} F^2 W = 0, \quad (6)$$

$M(F)$ is twice the mean curvature of the interface, that is:

$$M(F) = \frac{F \left[1 + (F_z)^2 \right] \left[F_{\theta\theta} - F \right]}{\left\{ F^2 \left[1 + (F_z)^2 \right] + (F_\theta)^2 \right\}^{3/2}} + \frac{F F_{zz} \left[F^2 + (F_\theta)^2 \right] - 2 F_\theta \left[F_\theta + F F_z F_{z\theta} \right]}{\left\{ F^2 \left[1 + (F_z)^2 \right] + (F_\theta)^2 \right\}^{3/2}}.$$

Boundary conditions are:

$$F(\pm \Lambda, \theta) = \left[(1 \pm h)^2 - e^2 \sin^2 \theta \right]^{1/2} \pm e \cos \theta, \quad (7)$$

$$F(z, \theta + 2\pi) = F(z, \theta), \quad (8)$$

$$\frac{1}{2} \int_{-\Lambda}^{\Lambda} dz \int_0^{2\pi} F^2 d\theta = 2\pi \Lambda V. \quad (9)$$

To write down the above expressions all lengths have been made dimensionless with $R_0=(R_1+R_2)/2$; $F=F(z, \theta)$

stands for the shape of the interface, and the parameters appearing in the problem formulation have been already defined. P is a constant related to the difference between the outer pressure and the inner pressure which has been made dimensionless with σ/R_0 . The subscripts z and θ indicate derivatives with respect to z and θ , respectively.

Equilibrium interface shapes are obtained by integration of the above formulation, expressions (6)-(9). In the general case, when the liquid bridge configuration is not axisymmetric, the integration of the problem (6)-(9) is very complicated, and only a few methods to calculate the liquid bridge interface have been reported [57, 58, 62]. Of course the integration methods developed for the non-axisymmetric case are of application to the axisymmetric one, but in the later (that means $B_r=e=0$), since derivatives with respect to the variable θ are zero, the problem formulation is drastically simplified to:

$$M(F) + P - B_a z + \frac{1}{2} F^2 W = 0, \quad (10)$$

$$M(F) = \frac{1}{\left[1 + (F_z)^2\right]^{3/2}} \left[F_{zz} - \frac{1 + (F_z)^2}{F} \right],$$

$$F(\pm A) = (1 \pm h)^2, \quad (11)$$

$$\int_{-A}^A F^2 dz = 2AV, \quad (12)$$

which is much more simple to handle. In this case, the system (10)-(12) can be integrated by using shooting methods like the one described in [36]. If no body forces are considered ($B_r=W=0$) the problem formulation reduces even more (differential equation becomes $M(F)+P=0$) and the equilibrium interface shapes can be expressed in terms of elliptic integrals [22].

In the case of almost cylindrical volume liquid bridges ($V=1$), assuming that all the parameters involved in the problem formulation (except the slenderness) are small enough, it is possible to obtain an approximate analytical expressions for the equilibrium interface

shape of liquid bridges starting from a known solution (the cylinder) and considering different kind of stimuli. In this case the configuration of reference to be perturbed is a cylindrical volume liquid bridge ($v=V-1=0$) held between equal in diameter, coaxial disks and in absence of body forces ($e=h=B_a=B_r=W=0$). This configuration of reference has the well known solution $F=1$, $P=1$. A solid body rotation ($W \neq 0$) could also be considered and the basic solution will still be a cylinder [51]. If now we consider a situation where the different parameters under consideration are not zero, but small, the expression for the liquid bridge interface can be expanded in the above quoted parameters, as follows:

$$F(z, \theta) = 1 + \sum_i \varepsilon_i f_i(z, \theta) + \sum_i \sum_j \varepsilon_i \varepsilon_j f_{ij}(z, \theta) + \dots, \quad (13)$$

$$P(z, \theta) = 1 + \sum_i \varepsilon_i p_i(z, \theta) + \sum_i \sum_j \varepsilon_i \varepsilon_j p_{ij}(z, \theta) + \dots, \quad (14)$$

where ε_i , ε_j stand for the different small parameters.

A general asymptotic solution for the approximate equilibrium shapes of liquid bridges without solid body rotation ($W=0$) was obtained in [40], although in that work the variable $S=F^2$ was used instead of F . An asymptotic expression giving directly the function F has been published later in [63].

As already explained, in the floating zone problem the more relevant parameters are the axial Bond number and the radii ratio of supporting disks, and, to less extent, the Weber number. The other two remaining parameters, lateral Bond number and eccentricity, are of much less importance (crystals are tried to be grown vertically and the supports are tried to be coaxial, as already said). In the floating zone case, where liquid configurations are axisymmetric but no longer cylinders, to calculate equilibrium interface shapes the shooting methods already quoted are of application.

However, to get some insight of the relationship between interface shape and stability it is worth to obtain an approximate expression for the liquid bridge interface. Therefore, the scope of the following analysis is restricted to the influence of $v=V-1$, h and B_a , according to reference [63] and the value of these three parameters is considered to be small enough. Under these assumptions the equilibrium interface shape can

be expressed as:

$$F(z) = 1 + \nu f_1 + B_a f_2 + h f_3 + \nu^2 f_{11} + B_a^2 f_{22} + h^2 f_{33} + 2(\nu B_a f_{12} + \nu h f_{13} + B_a h f_{23}), \quad (15)$$

where the nine functions f_i, f_{ij} are:

$$f_1 = \frac{1}{2} N (\cos z - \cos \Lambda),$$

$$\text{where } N = \frac{\Lambda}{\sin \Lambda - \Lambda \cos \Lambda},$$

$$f_2 = z - \Lambda \frac{\sin z}{\sin \Lambda},$$

$$f_3 = \frac{\sin z}{\sin \Lambda},$$

$$f_{11} = T_{11}(z) - T_{11}(\Lambda),$$

$$f_{12} = T_{12}(z) - T_{12}(\Lambda) \frac{\sin z}{\sin \Lambda},$$

$$f_{13} = T_{13}(z) - T_{13}(\Lambda) \frac{\sin z}{\sin \Lambda},$$

$$f_{22} = T_{22}(z) - T_{22}(\Lambda),$$

$$f_{23} = T_{23}(z) - T_{23}(\Lambda),$$

$$f_{33} = T_{33}(z) - T_{33}(\Lambda),$$

the functions $T_{ij}(z)$ being:

$$T_{11}(z) = \frac{1}{8} N^2 \sin^2 z + \frac{1}{4} N^2 \cos \Lambda [(2 - N \Lambda \sin \Lambda) \cos z - z \sin z],$$

$$T_{12}(z) = \frac{1}{4} N \left(\frac{1}{2} z^2 \sin z - 2z \cos \Lambda \right) + \frac{N \Lambda \cos z}{4 \sin \Lambda} (\sin z - z \cos \Lambda),$$

$$T_{13}(z) = \frac{N \cos z}{4 \sin \Lambda} (z \cos \Lambda - \sin z),$$

$$T_{22}(z) = \frac{\Lambda \cos z}{2 \sin \Lambda} (4 - \Lambda^2 + z^2) + \frac{\Lambda^2 \cos^2 z}{2 \sin^2 \Lambda} + z^2,$$

$$T_{23}(z) = -\frac{\cos z}{4 \sin \Lambda} (4 - \Lambda^2 + z^2 - 2N \Lambda \sin \Lambda) - \frac{\Lambda \cos^2 z}{2 \sin^2 \Lambda},$$

$$T_{33}(z) = \frac{\cos^2 z}{2 \sin^2 \Lambda} - \frac{1}{2} N \cos z$$

(there is a misprint in the expression of $T_{33}(z)$ in [63], where $\cos^2 z / \sin^2 \Lambda$ must be read instead of $\cos^2 z / \sin^2 z$).

Note that in the above expression the functions f_1 and f_{11} are symmetric with respect to the middle plane parallel to the disks (that means that $f(z) = f(-z)$), whereas the others are antisymmetric ($f(z) = -f(-z)$). In consequence, at least within the range of validity of this asymptotic analysis, any variation of the liquid bridge volume with respect to the cylindrical volume causes a symmetric deformation of the liquid bridge interface (interface bulging or necking at the centre of the liquid column is obtained depending on the sign of ν). On the other hand the interface deformation due to both the axial Bond number and the radii ratio of the supporting disks causes the bulging of one half of the liquid column and the necking of the other, and since the deformations due to each one of the parameters involved, h and B_a , can be in phase or in counter-phase, in the former case the necking effect will be accentuated (that means to be closer to stability loss, as explained in the following), whereas in the second both effects can compensate or even cancel each other. Therefore (see Fig. 3), liquid bridges between unequal disks are less stable when gravity points towards the larger disk (right sketch) than when it points towards the smaller one (left sketch).

4. STABILITY OF AXISYMMETRIC BASIC CONFIGURATIONS

The simplest non-trivial (non-cylindrical) liquid-bridge configuration consists of an axisymmetric, isothermal drop of liquid spanning between two parallel, coaxial, equal in diameter, solid disks, in absence of body forces

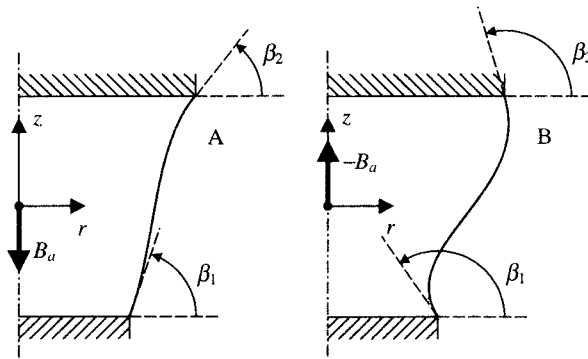


Fig. 3. Interface shape of liquid bridges between unequal disk. Because of necking effects configuration B is less stable than configuration A.

($e=h=B_a=B_l=W=0$). Early stability studies concerning basic configurations were published some three decades ago. The most relevant results concerning the stability of such configurations were published in the decade of the seventies and early eighties (see Table 2).

The stability diagram for axisymmetric liquid bridges with $e=h=B_a=B_l=W=0$ is shown in Fig. 4. The maximum volume of an axisymmetric liquid bridge (curve OD) is determined by the appearance of a non-axisymmetric perturbation which causes a non-axisymmetric bulging deformation of the liquid bridge interface and a (possibly not reversible) spreading of the liquid over the lateral surfaces of the supporting disks, whereas the smaller possible value of the volume (the minimum volume stability limit) is driven for most of the points (curve A-B-C) by an axisymmetric perturbation whose nature depends on the slenderness. Still in the lower part, and for very short liquid bridges (curve O-A), the destabilizing perturbation is non-axisymmetric.

For relatively large values of the slenderness, $A > 2.128$, the minimum volume stability limit is determined by the appearance of a catastrophic pitchfork bifurcation to non-symmetric (with respect to the middle plane parallel to the disks) unstable equilibrium shapes (indeed the corresponding eigenfunction is antisymmetric with respect to the middle plane). On the other hand, for moderate or small values of the

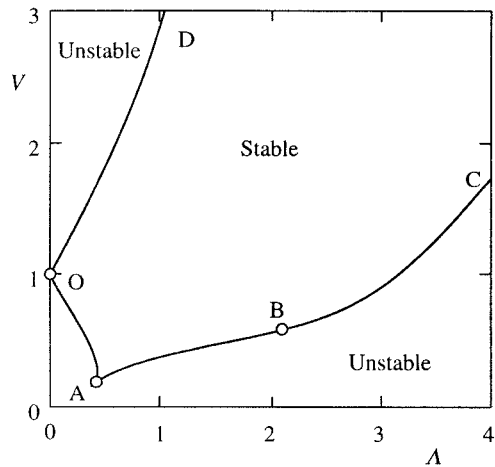


Fig. 4. Stability diagram of axisymmetric liquid bridges between coaxial, equal disks under zero gravity conditions ($e=h=B_a=B_l=W=0$).

slenderness, $A < 2.128$, the stability limit is determined by a turning point in the bifurcation diagram and the associate unstable equilibrium shapes are still symmetric with respect to the middle plane parallel to the disks [22, 28]. If the slenderness is small enough there is another constraint fixing the minimum volume of the liquid column: a non-axisymmetric instability

appears and, depending on the contact angle, a possible detachment of the liquid bridge interface from the edges of the disks could happen.

5. UNEQUAL DISKS AND AXIAL BOND NUMBER

Although the interest on the influence of several types of stimuli and of liquid bridge geometries different from the cylindrical one has paid the attention of many scientists during the last three decades, early publications on these topics were concerned only with partial aspects of the Λ - V stability diagram. The complete stability diagrams, considering all parts of the stability limits (both minimum volume and maximum volume), of liquid bridges between unequal disk radii, in zero gravity conditions or subjected to body forces (including solid body rotation) have only been published recently [34, 44]

Concerning the influence of axial Bond number, early studies were concerned with the maximum stable slenderness of liquid bridges between equal disks having cylindrical volume ($V=1$). Different attempts have been made to calculate the minimum volume stability limit as well as the maximum volume stability limit both from the theoretical [30, 31, 32] and experimental point of view [30, 33]. This problem has been extensively analysed in a work published at the beginning of the nineties [34]. A typical stability limit curve is presented in Fig. 5 ($e=h=B_f=W=0$, $B_a=1$). As can be seen, for any non zero value of the axial Bond number the stability limit can be represented by a single closed curve in the Λ - V plane. In the stability limit it is possible to distinguish, as in the previous case for zero gravity, three different parts. For small volumes and small slenderness the instability is governed by a non-axisymmetric instability and a possible detachment of the interface from the edge of the top disk. Another part of the stability limit is characterised by the axisymmetric breakage of the liquid column (that part corresponds to the minimum volume for moderate to large slendernesses) whereas the last (upper) part of the limit is characterised by the loss of axisymmetry of the equilibrium shapes and the appearance of non-axisymmetric bulging deformations of the interface (maximum volume stability limit). Nevertheless, if axial Bond number is large enough ($B_a > 3.07$) all destabilising perturbations are non-axisymmetric.

In most of the references quoted in Table 2 stability

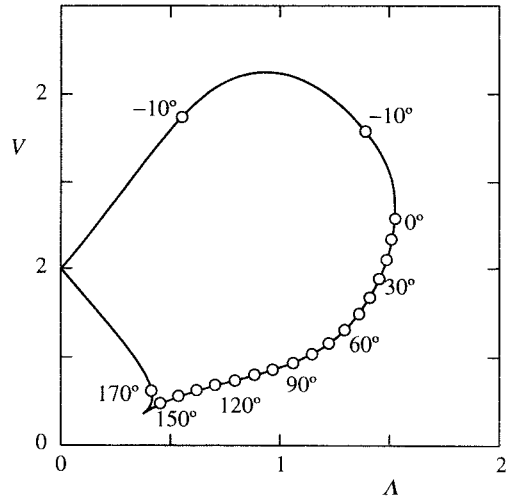


Fig. 5. Stability diagram of axisymmetric liquid bridges between coaxial, equal disks, without solid body rotation ($e=h=B_f=W=0$) subjected to an axial Bond number $B_a=1$. Numbers on the curve indicate the value of the angle β_1 .

diagrams in the plane Λ - V are defined by the appearance of different types of instabilities, either axisymmetric or non-axisymmetric, as discussed above. However, this approach, based on a strict mathematical formalism, yields in some cases to limiting liquid bridge interfaces that are extremely far from those usually appearing in floating zone technique. To clarify further this statement, in Fig. 5 the values of the angle β_1 along the stability limit curve corresponding to the case $B_a=1$, $K=1$ are shown. Observe that, at the stability limit curve, the angle β_1 can be negative or very close to 180° , depending on the values of both the slenderness and the volume (the same happens with β_2). Obviously these cases have not physical meaning from the point of view of the floating zone technique (this would imply that the interface enters in the solid rods as could be deduced from the sketches in Fig. 3), and the limiting curves to be considered in practice should be rather different. In an extreme situation, assuming that the molten interface is parallel at each one of the supporting rods to the solid-liquid interface, the limiting values of the angles β_1 and β_2 would be the angles formed by the protruding caps existing at the

melting front and at the solidification front. Even this case is a too severe constraint, the zone of interest for crystal growers being the part of the stability limit curve where β_1 is close, but smaller than 90° .

Additional insight on the region of interest in the Λ - V plane can be obtained by plotting over the stability diagram the lines $\beta_1 = \text{constant}$. In Fig. 6 the lines $\beta_1 = \text{constant}$ corresponding to liquid bridges between equal disks subjected to an axial Bond number ($B_a = 0.01$) have been represented. The values of β_1 have been calculated under the assumption that the liquid bridge volume is almost cylindrical and that the Bond number is small enough, so that equation (15) has been used to calculate the liquid bridge interfaces. Note that for the value of the Bond number under consideration the region of volumes of interest lies near $V=1$, but with volumes smaller than the cylindrical one.

As already said the stability limits of liquid bridges

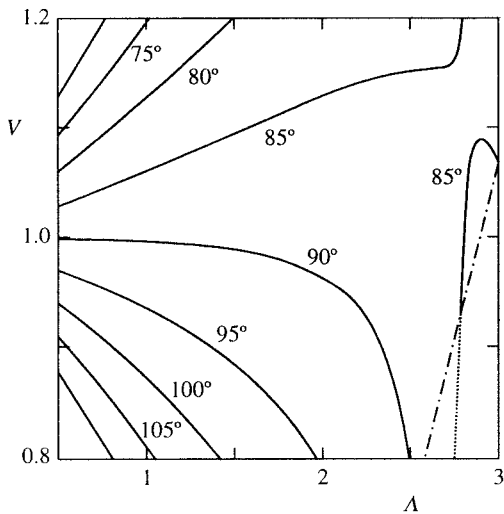


Fig. 6. Variation with the slenderness, Λ , and the liquid bridge volume, V , of the angle β_1 formed by the liquid bridge interface at the bottom disk. The results have been obtained by using the approximation for the liquid bridge interface given by equation (15) and correspond to axisymmetric liquid bridges between coaxial, equal disks, without solid body rotation ($e=h=B_f=W=0$) subjected to an axial Bond number $B_a=0.01$. Dot-dashed line is the stability limit.

between equal disks is an thoroughly analysed problem, the agreement between available experimental and theoretical results being excellent. In Fig. 7 experimental results on the variation with the Bond number of the absolute maximum slenderness, Λ_{MAX} , of liquid bridges between equal disks is compared with theoretical predictions (be aware that, if the value B_a is small enough, the absolute maximum slenderness will be reached for quite large values of the liquid bridge volume). The discrepancies shown for small values of B_a can be attributed to other uncontrolled disturbances in the experiments.

The influence on stability limits of having disks with different diameters has been mainly investigated in the last two decades. At the beginning the efforts were concentrated mainly on the stability limits of minimum volume [35, 36]. The problem of the calculation of the maximum volume of liquid bridges between unequal disks has been reported quite recently [37]. The influence of unequal disks in the Λ - V stability diagram is shown in Fig. 8. Only the relevant part of the diagram (minimum volume limit and small to moderate values of the slenderness) has been plotted. As it can be observed the stable region in the Λ - V plane decreases as the parameter K decreases (h increases).

The combined influence of both unequal disks and axial

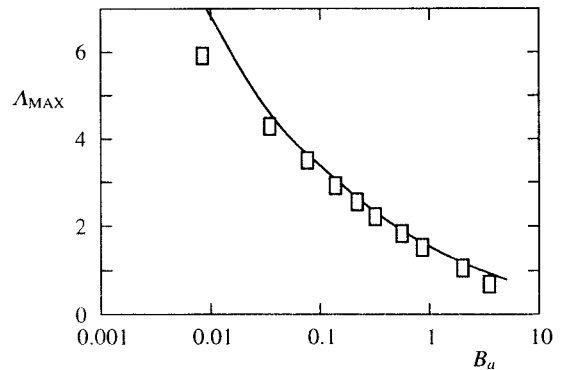


Fig. 7. Variation with the axial Bond number B_a of the absolute maximum slenderness, Λ_{MAX} , of axisymmetric liquid bridges between coaxial, equal disks, without solid body rotation ($e=h=B_f=W=0$). Solid line represents theoretical results from [34] whereas symbols correspond to experimental ones from [33].

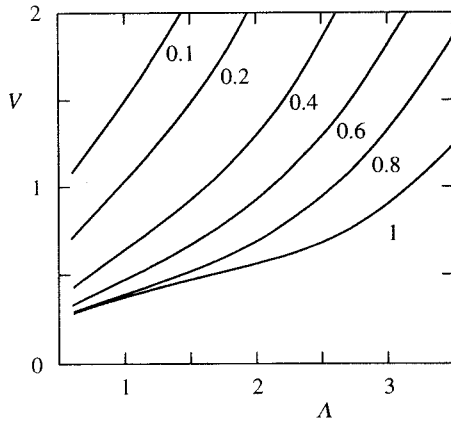


Fig. 8. Stability diagram of axisymmetric liquid bridges between coaxial, unequal disks under gravitationless conditions and without solid body rotation ($e=B_a=B_l=W=0$, $K \neq 1$). Numbers on the curves indicate the value of the parameter K (from [35]).

Bond number on stability limits of minimum volume was first studied through a bifurcation analysis by the mid eighties [38]. According to this study, the maximum stable slenderness, Λ_{\max} , of a liquid bridge of almost cylindrical volume ($v=V-1 \ll 1$), between disks of different radii ($h \ll 1$), and subjected to an axial Bond number ($B_a \ll 1$), is given by the expression:

$$\frac{\Lambda_{\max}}{\pi} = 1 - \left(\frac{3}{2}\right)^{4/3} \left(B_a - \frac{h}{\pi}\right)^{2/3} + \frac{1}{2}v \quad (16)$$

According to equation (16), if the effect of axial gravity and the effect of unequal disks are considered separately, each one of them reduce the stable region (as can be observed in Figs. 5 and 8). Nevertheless, since both effects are non-symmetric with respect to the middle plane parallel to the disks, under certain circumstances (when they are in opposition) they can compensate to a certain extent (this happens when axial gravity is directed towards the smaller disk).

The more comprehensive results up to now published on the combined influence of both $h \neq 0$ and $B_a \neq 0$ can be found in [43], where the minimum volume stability limits are analysed both theoretically and experimentally, and in [44] where the complete stability

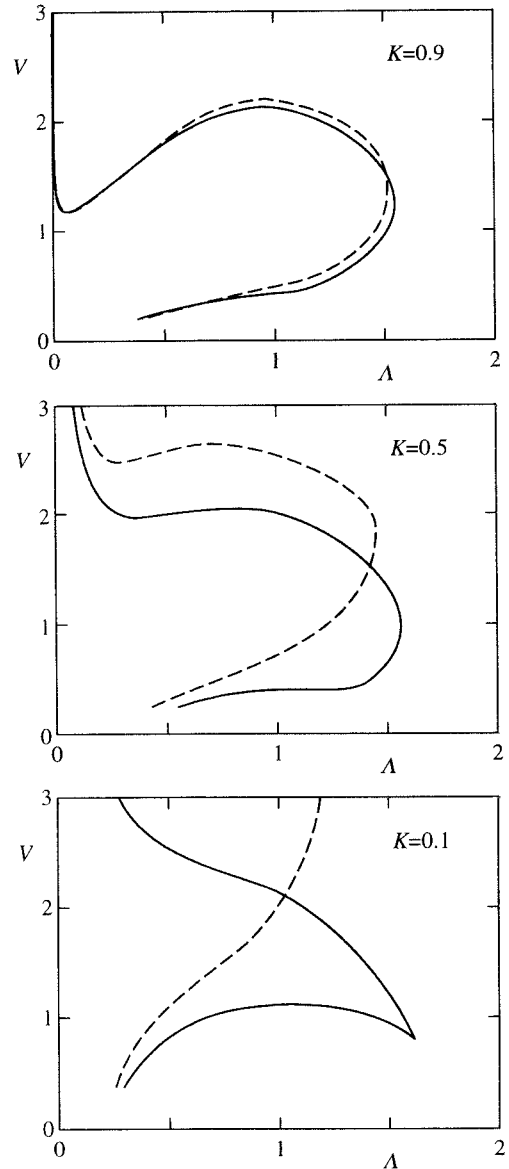


Fig. 9. Stability diagrams of axisymmetric liquid bridge between coaxial, unequal disks, without solid body rotation ($e=B_l=W=0$, $B_a \neq 0$, $h \neq 0$). Solid (dashed) lines correspond to a value of the axial Bond number $B_a=1$ ($B_a=-1$), (from [44]).

diagrams are calculated. Typical sets of curves of stability limits are shown in Fig. 9. As it can be observed, when both disks are not of the same diameter, the stability limit corresponding to a positive value of axial Bond number provides (in the range of values of interest) a stable region larger than that corresponding to $B_a=0$, showing the stabilising effect of axial Bond number in this case.

Available experimental results are in agreement with theoretical predictions [42, 43]. In Fig. 10. experimental results [42] concerning the stability limits of axisymmetric liquid bridge between coaxial, unequal disks ($K=0.6$), without solid body rotation ($e=B_f=W=0$) subjected to an axial Bond number B_a are compared with theoretical ones. Observe the large change of the stability limit curve depending on the sense of the axial Bond number (the liquid bridge is much more stable when gravity point towards the smaller disk).

6. SOLID BODY ROTATION

The case of the stability of a liquid column between equal disks, with cylindrical volume and in gravitationless conditions ($e=h=B_a=B_f=0$, $V=1$) was first analysed almost twenty years ago. As it is well known the nature of the instability appearing when the liquid bridge rotates as a solid body depends on the value of

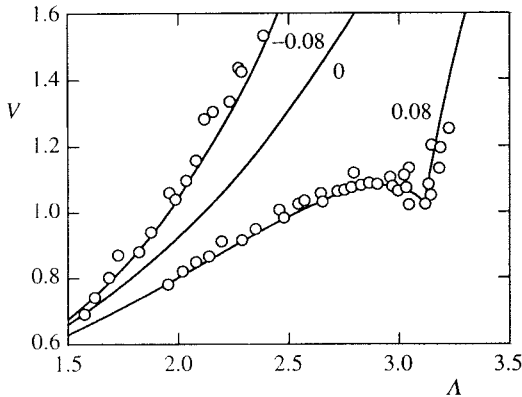


Fig. 10. Stability diagrams of axisymmetric liquid bridge between coaxial, unequal disks ($K=0.6$), without solid body rotation ($e=B_f=W=0$). Symbols indicate experimental results (from [42]). Numbers on the curves indicate the value of the axial Bond number B_a .

Weber number. According to the linear stability analysis [51], for low values of the Weber number, $W \leq 1/3$, the loss of stability of a cylindrical equilibrium shape is due to axisymmetric perturbations (amphora mode), the maximum stable slenderness being $\Lambda_{\max} = \pi(1+W)^{-1/2}$. On the other hand, if the value of Weber number is large enough, $W \geq 1/3$, the stability loss is due to non-axisymmetric perturbations, and the so-called "C-mode" develops. In this second case the maximum stable slenderness becomes $\Lambda_{\max} = \pi/(2W)$.

With respect to the combined effect of both Weber number and axial Bond number, available results demonstrate that within the range of validity of an asymptotic analysis (values of the Weber number close to the critical one and small values of the Bond number [51]) the maximum stable slenderness of an axisymmetric liquid bridge ($e=B_f=0$) between equal disks ($h=0$) and cylindrical volume ($V=1$) becomes:

$$\Lambda_{\max} = \frac{\pi}{(1+W)^{1/2}} \left[1 - \left(\frac{9B_a}{4(1+W)^{5/2}} \right)^{2/3} \right]. \quad (17)$$

The more general problem ($e=h=B_f=0$, $V \neq 1$, $B_a \neq 0$, $W \neq 0$) has been extensively studied in a recently published paper [52]. The results corroborate the behaviour predicted by equation (17): in the case of minimum volume stability limits solid body rotation decreases the stability region in the Λ - V plane no matter the particular liquid bridge configuration considered.

To our knowledge, leaving apart some experimental results on the effect of both unequal disk radii and solid body rotation that were published in the seventies [54, 55], the only (theoretical) available results on the combined effects of axial gravity, unequal disk radii and solid body rotation have been published in [53], although these results are only concerned with the minimum volume stability limit and they are limited to liquid bridges between almost equal disks ($h \leq 0.1$) and subjected to very small axial Bond numbers ($|B_a| \leq 0.05$). Additional theoretical and experimental efforts are clearly needed to fully understand the coupling between the different perturbations.

7. NON-AXISYMMETRIC PERTURBATIONS

As it has been already said, non-axisymmetric stimuli (lateral Bond number and eccentricity) are effects that

have a minor impact on floating zone processing on earth, although these effects can be of paramount importance in crystal growth in space platforms, where the other perturbation effects can be of the same order and the direction of gravity cannot be easily guessed beforehand (the direction with regard to the experimental facility can even change with time). The maximum stable slenderness of a cylindrical liquid bridge between equal disks subjected to a lateral Bond number ($e=h=B_a=0$, $V=1$, $B_l \neq 0$) was first analysed in [56], and the general case ($V \neq 1$) is analysed in [57, 58, 59, 60]. The combined effects of both $B_l \neq 0$ and $e \neq 0$ are analysed in [61, 62].

For the purposes of this paper, to understand how non-axisymmetric stimuli affect the stability of liquid bridges it is enough with some asymptotic results. In [64] an analytical expression of the maximum stable slenderness of liquid bridges with volume close to the cylindrical one and slenderness close to π , including both axisymmetric and non-axisymmetric stimuli, was calculated. According to this study the maximum stable slenderness become:

$$\frac{\Lambda_{\max}}{\pi} = 1 - \left(\frac{3}{2}\right)^{4/3} \left(B_a - \frac{h}{\pi} - \frac{3}{2\pi} B_l e \cos \beta \right)^{2/3} + \frac{1}{2}(V-1) - \frac{\pi^2}{4} B_l^2 - \frac{3}{4\pi^2} e^2. \quad (18)$$

Obviously, equation (18) is only of application to liquid bridge configurations close to the reference one ($e=h=B_a=B_l=0$, $V=1$), but allows us to deduce more general conclusions concerning the influence on the stability limit of the perturbations under consideration. For instance, within this approximation, there is not coupling between the different effects on the variation of the critical slenderness but between B_l and e and, when these two effects are considered, another important feature pointed out by equation (18) is that Λ_{\max} does depend on the angle β between the plane defined by the axes of the disks and the direction of the lateral component of microgravity. This behaviour is clearly shown in Fig. 11.

Another important characteristic of the stability of liquid bridges that must be remarked is that the combined effect of both lateral Bond number and eccentricity (the term in $B_l e$) can be a stabilizing factor

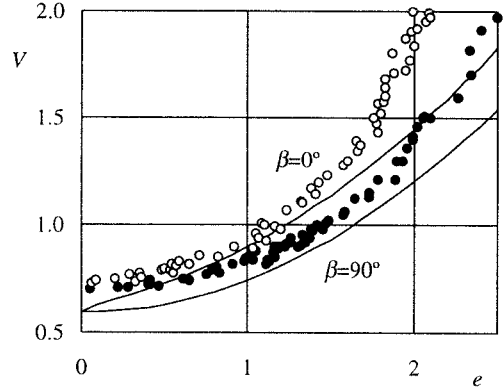


Fig. 11. Minimum volume of the liquid bridge, V , versus eccentricity, e , of liquid bridges between equal disks with slenderness $\Lambda=2.5$ subjected to a lateral Bond number $B_l=0.02$. The symbols represent experimental results from [64]. Solid lines indicate theoretical results according to expression (18).

for the liquid column. Observe that, besides the combined effect of axial Bond number and unequal disks, in the case of non-coaxial disks the liquid bridge can be more stable if the acceleration has both axial and lateral components than if only one of them is acting on the liquid bridge.

The reason for this behaviour lies again on the deformation of the liquid column. When $B_l \neq 0$ and $e \neq 0$, provided $\beta \neq \pi/2$, the lateral acceleration tends to bulge the liquid bridge close to the disk that is in the direction toward lateral acceleration points and to neck the liquid interface at the opposite one. If axial acceleration is then oriented towards the disk where the liquid bridge bulges, both effects, axial acceleration and the combination of lateral acceleration plus eccentricity, act in the same sense, so that the bulging effect is accentuated (and in consequence the necking one). In this case the stability is decreased.

Obviously, the reasoning is just the opposite when the interface deformation caused by axial acceleration is in opposition to that due to the combination of lateral acceleration and eccentricity, and in this case the resulting configuration is more stable than the configuration obtained when only one of these two groups of effects are considered.

CONCLUSIONS

In this paper a brief review on the stability limits of liquid bridges under a wide variety of stimuli, either axisymmetric or non-axisymmetric, has been presented. Out of a huge work of many authors in the last thirty years, a subset of results, particularly relevant for the floating zone technique has been extracted and presented.

The effects reviewed are not all that have been considered in the literature. There are other stimuli whose effects on stability limits have been analysed, mainly the influence of electric and magnetic fields, but these are out of the scope of this review.

ACKNOWLEDGEMENT

This work has been supported by the Spanish Comisión Interministerial de Ciencia y Tecnología (CICYT).

REFERENCES

- [1] Hurlle, D.T.J. 1981, *Adv. Colloid Interface Sci.*, 15, 101.
- [2] Eyer, A., Kolbesen, B.O., and Nitsche, R. 1982, *J. Crystal Growth*, 57, 145.
- [3] Wilcox, W.R. 1984, *Encyclopedia of Chemical Technology*, vol. 24, John Wiley and Sons, 903
- [4] Tatarchenko, V.A. 1977, *J. Crystal Growth*, 37, 272.
- [5] Tatarchenko, V.A., and Satunkin, G.A. 1977, *J. Crystal Growth*, 37, 285.
- [6] Boucher, E.A., and Evans, M.J.B. 1985, *J. Chem. Soc. faraday Trans. 1*, 85, 2787.
- [7] Martínez, I., and Eyer, A. 1986, *J. Crystal Growth*, 75, 535.
- [8] Martínez, I., and Cröll, A. 1992, *ESA SP-333*, 135
- [9] Sanz, A. 1991, *Microgravity Fluid Mechanics*, H.J. Rath (Ed.), Springer-Verlag, Berlin, 3
- [10] Meseguer, J., Slobozhanin, L.A., and Perales, J.M. 1994, *Adv. Space Res.* 16, 5.
- [11] López-Díez, J. 1991, *Microgravity Sci. Technol.*, III/4, 222.
- [12] Martínez, I., Sanz, A., Perales, J.M., and Meseguer, J. 1988, *ESA Journal*, 12, 483.
- [13] Gonzalez, H., Mc Cluskey, F.J.M., Castellanos, A., and Barrero, A. 1989, *J. Fluid Mech.*, 206, 545.
- [14] Ramos, A., and Castellanos, A. 1993, *J. Fluid Mech.*, 249, 207.
- [15] González, H., and A. Castellanos, A. 1993, *J. Fluid Mech.*, 249, 185.
- [16] Mahajan, M.P., Tsinge, M., Taylor, P.L., and Rosenblatt, C. 1998, *Phys. Fluids*, 10, 9.
- [17] Mahajan, M.P., Zhang, S., Tsinge, M., Taylor, P.L., and Rosenblatt, C. 1999, *J. Coll. Interface Sci.* 123, 592.
- [18] Haynes, J.M. 1970, *J. Colloid Interface Sci.* 32, 652
- [19] Erle, M.A., Gillette, R.D., and Dyson, D.C. 1970, *Chem. Eng. J.*, 1, 97.
- [20] Mason, G.C. 1970, *J. Colloid Interface Sci.*, 32, 172.
- [21] Gillette, R.D., and Dyson, R.C. 1971, *Chem. Eng. J.*, 2, 44.
- [22] Martínez, I. 1978, *COSPAR Space Research XVIII*, M.J. Rycroft and A.C. Stickland (Eds.), Pergamon Press, Oxford, 519.
- [23] Da Riva, I., and Martínez, I. 1979, *SP-142*, 67.
- [24] Sanz, A., and Martínez, I. 1983 *J. Colloid Interface Sci.*, 93, 235.
- [25] Russo, M.J., and Steen, P.H. 1986, *J. Colloid Interface Sci.* 113, 154.
- [26] Boucher, E.A., and T.G. Jones, T.J. 1988, *J. Colloid Interface Sci.*, 126, 469.
- [27] Lowry, B.J., and Steen, P.H. 1995, *Proc. R. Soc. London A*, 449,441.
- [28] Slobozhanin, L.A., Alexander, J.I.D., and Resnick, A.H. 1997, *Phys. Fluids*, 9, 1893
- [29] Boucher, E.A., and Evans, M.J.B. 1980, *J. Colloid Interface Sci.*, 75, 409.
- [30] Meseguer, J., and Sanz, A. 1985, *J. Fluid Mech.* 153, 83.
- [31] Martínez, I., Haynes, J.M., and Langbein, D. 1987, *Fluid Sciences and Material Science in Space*, H.U. Walter (Ed.), Springer-Verlag, Berlin, 53
- [32] Langbein, D. 1990, *J. Crystal Growth* 104, 47.
- [33] Bezdeneznykh, N.A., Meseguer, J., and Perales, J.M. 1992, *Phys. Fluids A*, 4, 677.
- [34] Slobozhanin, L.A., and Perales, J.M. 1993, *Phys. Fluids A*, 5, 1305.
- [35] Martínez, I. 1983, *ESA SP-191*, 267.
- [36] Martínez, I., and Perales, J.M. 1986, *J. Crystal Growth* 78, 369.
- [37] Slobozhanin, L.A., Gómez, M., and Perales, J.M. 1995, *Microgravity Sci. Technol.*, VIII/1, 23
- [38] Meseguer, J. 1984, *J. Crystal Growth* 67, 141

- [39] Meseguer, J. 1985, *J. Crystal Growth*, 73, 599.
- [40] Meseguer, J., Mayo, L.A., Llorente, J.C., and Fernández, A. 1985, *J. Crystal Growth*, 73, 609.
- [41] Meseguer, J., Sanz, A., and Perales, J.M. 1990, *Appl. Microgravity Tech.*, II/4, 186.
- [42] Bezdeneznykh, N.A., and Meseguer, J., 1991, *Microgravity Sci. Technol.*, IV/4, 235
- [43] Perales, J.M., Meseguer, J., and Martínez, I. 1991, *J. Crystal Growth*, 110, 855.
- [44] Slobozhanin, L.A., and Alexander, J.I.D. 1998, *Phys. Fluids*, 10, 2473
- [45] Brown, R.A., and L.E. Scriven, L.E. 1980, *Phil. Trans. R. Soc. Lond. A*, 297, 51.
- [46] Da Riva, I., 1981, *Applications of Space Technology*, Pergamon Press. Oxford, 69.
- [47] Perales, J.M., Sanz, A., and Rivas, D. 1990, *Appl. Microgravity Technol.* 2, 193.
- [48] Slobozhanin, L.A., and Perales, J.M. 1996, *Phys. Fluids*, 8, 2307
- [49] Coriell, S.R., and Cordes, M.R. 1977, *J. Crystal Growth*, 42, 466
- [50] Ungar L.H., and Brown, R.A. 1982, *Phil. Trans. R. Soc. Lond. A* 306, 347.
- [51] Vega, J.M., and Perales, J.M. 1983, *ESA SP-191*, 247.
- [52] Slobozhanin, L.A., and Alexander, J.I.D. 1997, *Phys. Fluids*, 9, 1880
- [53] Martínez, I., Perales, J.M., and M. Gómez, M. 1992, *ESA SP-333*, 123.
- [54] Carruthers, J.R., and Grasso, M. 1972, *J. Appl. Phys.*, 43, 436.
- [55] Carruthers, J.R., and Grasso, M. 1972, *J. Crystal Growth*, 13/14, 611.
- [56] Coriell, S.R., Hardy, S.C., and Cordes, M.R. 1977, *J. Colloid Interface Sci.*, 60, 126
- [57] Laverón-Simavilla, A., and J.M. Perales, J.M. 1995, *Phys. Fluids* 7, 1204.
- [58] Alexander, J.I.D., Delafontaine, S., Resnick, A., and Carter, W.C. 1996, *Microgravity Sci. Technol.* IX/3, 193.
- [59] Bezdeneznykh, N.A., Meseguer, J., and Perales, J.M. 1999, *Phys. Fluids*, in press.
- [60] Zayas, F., Alexander, J.I.D., and Meseguer, J. 1999, *Phys. Fluids*, submitted.
- [61] Perales, J.M. 1987, *Acta Astronautica*, 15, 561.
- [62] Laverón-Simavilla, A., and Checa, E. 1997, *Phys. Fluids* 9, 817
- [63] Meseguer, J., Bezdeneznykh, N.A., and Rodríguez de Francisco, P. 1996, *Microgravity Sci. Technol.*, IX/2, 62.
- [64] Meseguer, J., Bezdeneznykh, N.A., Perales, J.M., and Rodríguez de Francisco, P. 1995, *Microgravity Sci. Technol.*, VIII/1, 2.